Oehring, M.; Stark, A.; Paul, J.D.H.; Lippmann, T.; Pyczak, F.:

Microstructural refinement of boron-containing Beta-solidifying Gamma-titanium aluminide alloys through heat treatments in the Beta phase field

In: Intermetallics (2012) Elsevier

DOI: 10.1016/j.intermet.2012.08.010

Microstructural refinement of Boron containing β-solidifying γ-titanium aluminide alloys through heat treatments in the β phase field

M. Oehring, A. Stark, J.D.H. Paul, T. Lippmann and F. Pyczak

Helmholtz-Zentrum Geesthacht, Institute of Materials Research, Max-Planck-Str. 1,

D-21502 Geesthacht, Germany

Corresponding author: Michael Oehring, e-mail: michael.oehring@hzg.de,

Phone: +49 4152 87 2672, FAX: +49 4152 87 2534

e-mail-addresses: andreas.stark@hzg.de

jonathan.paul@hzg.de

thomas.lippmann@hzg.de

florian.pyczak@hzg.de

Abstract

The addition of B effectively supports the generation of fine and homogeneous microstructures in as-cast β-solidifying γ-based titanium aluminide alloys. The microstructural refinement in such alloys can be attributed to the borides acting as nucleation sites for new α grains during the solid-state $\beta \rightarrow \alpha$ transformation (Hecht U, Witusiewicz V, Drevermann A, Zollinger J, Intermetallics 2008; 16: 969-978). In the current work it is shown that the cooling rate plays a crucial role in determining whether borides serve as nucleation sites for grain refinement. Surprisingly, if the cooling rate is too high then grain refinement by borides is hampered. The positive effect of borides can be used to obtain grain refinement in these materials by a simple heat treatment, even if the microstructure has been extensively coarsened through prior heat treatment.

Keywords: A. titanium aluminides, based on TiAl. B. phase transformation. B. phase identification. C. crystal growth. D. microstructure.

1 Introduction

Current cast high-strength γ-TiAl alloys are superior to competing Ni-base superalloys with respect to specific strength up to a temperature of about 800 °C [1-3]. Unfortunately, these high-strength alloys suffer from reduced ductility and show a high sensitivity to processing conditions. A fine-grained microstructure without significant texture might provide the ductility necessary for the application of these alloys in safety relevant applications such as aero-engine components [4]. Such microstructures can be especially difficult to achieve via casting. Thus the majority of alloying strategies for such high-strength alloys are motivated by the desire to produce an alloy which develops a fine-grained, ductile and damage tolerant microstructure. These strategies include a reduction of the aluminum content, the addition of niobium and other β-stabilizing elements, as well as alloying with boron to benefit from grain refinement via the presence of borides [4, 5]. Through a combination of reduced Al-content and the addition of β-stabilizing elements it is possible to generate an alloy composition which solidifies via the β-single phase field. Naka et al. [6] were probably the first to clearly point out that such β-solidifying alloys offer significant potential for grain refinement. In parallel, the coarse-grained structure normally encountered in peritectically solidifying alloys was explained by Johnson et al. [7] and Küstner et al. [8] by the simultaneous growth of the β and α phases during solidification and a subsequent overgrowth of the primary β dendrites by the secondary α grains. In a β-solidifying alloy the microstructure formation after solidification is significantly different from the peritectic case. The complete solidification and phase transformation path of a β-solidifying alloy can be described as follows: liquid → β → β+α (→ α) → α+γ(+β) → α_2+γ(+β). Whether low temperature β phase and a single α-phase field exist depends on the exact alloy composition. Additionally, at lower temperatures the β phase may occur in its ordered variant β_o with the B2 crystal structure. Several authors have emphasized that the multitude of phase transformations involving the β phase in multi-component alloys might be used to obtain refined microstructures [9 - 15]. During the transformation of β to the α phase, Widmannstätten α-laths can crystallize in twelve different orientation variants from one parent β grain. All these twelve orientation variants obey the Burgers orientation relationship [5] - {110}β || (0001)α and <111>β || <11-20>α - with the initial β grain. In addition the single α-phase field in these alloys is either restricted or even fully absent so that α grain growth at lower temperatures is limited.

It is well known that further grain refinement in these alloys can be achieved by the addition of boron, forming TiB mono- or TiB_2 di-borides [16 - 18]. For a sufficiently high boron content and an

appropriate alloy composition these borides can exist up to the melting temperature of the alloy. On the contrary, in Al-lean TiAl-alloys with low boron content, borides are not stable in the melt. Therefore, they are not expected to play any role in the nucleation of the primary β phase from the melt. However, B strongly segregates to the melt during solidification and for this reason the segregation zone is highly constitutionally undercooled in comparison to B-free alloys which could result in a higher density of nucleation events of e.g. the β phase and thus B-induced microstructural refinement [17]. Furthermore, grain refinement by borides can take place during the subsequent solid-state phase transformation at lower temperatures. During the $\beta \rightarrow \alpha$ phase transformation, borides can act as nucleants for new α grains leading to a higher number of smaller α grains from one initial β grain. In the absence of borides, the β grain boundaries are thought to be the preferred nucleation sites of new α grains, as is the case for Ti alloys [19]. If precipitation of α at β grain boundaries occurs then the resulting microstructure has a lamellar appearance of Widmannstätten laths with different α grains growing from the prior β grain boundaries into the grain interior. Here it is worth mentioning that the β/α transformation often results in adjacent α grains having the same orientation [20]. Since γ lamellae are precipitated from the α phase exclusively with orientations according to the Blackburn orientation relationship, groups of neighboring lamellar colonies with the same lamellae orientation may arise. Thus, the refinement of the lamellar colony size obtained through the formation of Widmannstätten laths might not improve the mechanical properties of the materials [20] because the orientation distribution of γ lamellae also plays a significant role. Recently, Hecht et al. [5] have shown for cast β-solidifying alloys that the misorientations between adjacent α grains could be attributed to the Burgers orientation relationship with respect to the parent β phase in a B-free alloy. On the contrary the α phase formed with a random crystallographic orientation distribution in a B-containing alloy. This clearly indicates that in the latter case the mechanism of refinement is based on heterogeneous nucleation of α on the borides during the solid-state β/α transformation as suggested by Imayev et al. [9]. The work presented in the current paper demonstrates that not only the presence of borides, but also the cooling rate, has a strong influence on this solid-state β/α transformation and the microstructure that is formed. Investigations have been performed with both high-energy X-ray diffraction using a 2-dimensional detector, and with Electron Backscattered Diffraction (EBSD), on B-containing and B-free alloys which experienced different heat treatments and cooling conditions.

2 Materials and Methods

Alloys in the composition range Ti-(44-45)Al-(5-7)Nb-(0.5-1)Mo-(0-0.2)B (at.%) were chosen for the investigation. The material was produced as round 32 g buttons in a laboratory arc-melting furnace on a water-cooled copper plate under an Ar atmosphere. The buttons were melted at least 7 times to ensure sufficient homogeneity. Subsequent heat treatments were carried out under air in a muffle furnace. After heat treatment care was taken to remove the oxidised surface layer from the specimens before proceeding further.

Specimens for microstructural and analytical investigations were prepared from approximately 3 mm thick slices that were cut along the main axis of the round arc-melted buttons. For scanning electron microscopy these specimens were ground and subsequently electro-polished at -19 V and a temperature of -45 °C in a solution of 600 ml methanol, 300 ml n-butanol and 60 ml perchloric acid. Scanning electron microscopy was carried out using the back-scattering mode in a Zeiss DSM962 and a LEO Gemini 1530 microscope, the latter equipped with a field emission gun. For electron backscatter diffraction (EBSD) investigations a TSL analysis system fitted to the Gemini 1530 microscope was employed. The proprietary TSL software was used for EBSD data analysis. To avoid the removal of boride particles during electrolytic polishing some specimens for EBSD investigations were mechanically polished with a vibrating polisher. High-energy X-ray diffraction (HEXRD) experiments using synchrotron radiation were performed at the HARWI II beamline run by the Helmholtz-Zentrum Geesthacht at the Deutsches Elektronen-Synchrotron (DESY). HEXRD investigations were conducted in transmission at room temperature on the same specimen slices that had been used for microstructural analysis. The X-ray beam had a cross-section of 1 x 1 mm^2 and a photon energy of 100 keV, corresponding to a wavelength of $\lambda = 0.12398$ Å. The reflections were recorded by a mar555 flat panel detector. Differential scanning calorimetry (DSC) was carried out in order to determine phase transformation temperatures by employing a Netzsch Pegasus 404C heat flux calorimeter. The scans were performed with a heating rate of 20 K/min under an Ar atmosphere (99.9999 % purity).

3 Results and discussion

The microstructures of the B-containing and corresponding B-free alloys under investigation in this work were compared in the as-cast and in different heat-treated conditions. Scanning electron microscopy observations of the B-free alloy Ti-45Al-7Nb-1Mo (at.%) showed a similar microstructure to that of lamellar near-α or $\alpha + \beta$ Ti alloys after casting (Fig. 1a). This morphology

stems from the solid-state reactions $\beta \rightarrow \beta+\alpha \rightarrow \alpha \rightarrow \alpha+\gamma \rightarrow \alpha_2+\gamma$. In the first transformation, Widmannstätten α plates are precipitated from the β phase with different orientations with respect to the parent phase. This leads to the segregation of Ti, Nb and Mo in the remaining β phase. Due to this enrichment of relatively heavy elements, the β phase appears brightly in the back-scattered SEM micrographs. Subsequently, during the $\alpha \rightarrow \alpha+\gamma$ transformation, γ lamellae are formed within the α plates. Fig. 2a shows the corresponding microstructure in the as-cast condition for the B-containing Ti-45Al-7Nb-1Mo-0.1 at.% B alloy. The microstructure is similar in overall appearance but more refined and uniform compared to the B-free alloy. Microstructures similar to the ones shown in Figs. 1a and 2a have often been reported in γ(TiAl) cast alloys [5, 6, 8, 9] and indicate that solidification occurred solely via the β phase.

As the current investigation aims to clarify the effect of borides on α grain nucleation and refinement during the solid state β/α transformation, a similar microstructure in the B-containing and the B-free versions of the alloy Ti-45Al-7Nb-1Mo was generated by an appropriate heat treatment as a defined starting condition. Via DSC the α-transus and β-transus of all alloys investigated in this study were found to be in the range 1272 – 1307 °C and 1387 – 1442 °C, respectively. Both the alloys, Ti-45Al-7Nb-1Mo and Ti-45Al-7Nb-1Mo-0.1 B were annealed for 2 h in the single-phase α region at 1310 °C and then oil-quenched. After this heat treatment both alloys showed very coarse microstructures consisting almost completely of the α phase (Figs. 1b and 2b). Subsequently, both alloys (with a coarse initial single α phase microstructure) were subjected to a further heat treatment. The specimens were heated to 1450 °C, within the single-phase β field, and held at temperature for 1 h. In order to investigate the influence of the cooling rate on the β/α transformation, the specimens were cooled down from the single-phase β field either by relatively fast air or by a slower furnace cooling with an initial cooling rate of around 60 K/min. In the B-free alloy coarse microstructures were observed, irrespective of the cooling rate (Figs. 1c and 1d). These microstructures exhibited the same typical morphological features of the β decomposition path as already described above for the as-cast state. In particular, it should be mentioned that adjacent lamellar colonies separated by remaining β phase, often had the same lamellae orientation. Thus large regions with a uniform alignment of lamellae were present. In the B-containing alloy, a similar microstructure with extended regions of a single lamellae orientation only formed in the air-cooled material (Fig. 2c), while the furnace-cooled specimen showed rather small lamellar colonies with apparently nearly random lamellae orientations (Fig. 2d). Thus adjacent colonies did not exhibit parallel lamellae. Both the grain refinement and the more uniform distribution of orientations can be explained by the mechanism proposed by Hecht et al. [5], i.e.

heterogeneous nucleation of the α phase at borides during the β/α transformation, while the dependence on cooling rate is a novel finding of the present study. It must be emphasized that the heat treatment scheme applied in this study guarantees that the microstructural refinement observed and investigated in this publication can be solely ascribed to the solid-state β/α transformation.
The Widmannnstätten α-laths in commercial α/β Ti alloys generally exhibit crystallographic orientations according to the Burgers orientation relationship [21]. Gey and Humbert [22] have shown that in this case only misorientation angles of 10.5°, 60°, 60.8°, 63.3° and 90° can occur between the α laths originating from one parent β grain. Thus, the misorientation angle can be used to examine whether the α phase obeys the Burgers relationship with respect to the parent β phase. Using EBSD investigations Hecht et al. [5] determined the misorientation angle distribution. They showed that in a B-free alloy misorientation angles of around 10°, 60°, 70° and 90° were found between neighbouring α phase laths while in B-containing alloys the α phase exhibited a broad distribution of misorientation angles. The same method has been used in the present study to distinguish between nucleation of the α phase at grain boundaries/grain boundary allotriomorphs of the parent β phase and at borides. The EBSD investigations were performed on an alloy Ti-44.5Al-(5-7)Nb-(0.5-1)Mo-0.1B. This material was subjected to the same heat treatment and cooling schemes as described earlier for the two versions of Ti-45Al-7Nb-1Mo. SEM investigations showed very similar microstructures (Fig. 3) to those found in the Ti-45Al-7Nb-1Mo-0.1B alloy after the same heat-treatment/cooling schemes. This is also reflected in the phase distribution maps recorded by EBSD (Figs. 4b and 4e), which show smaller lamellar colonies for the furnace-cooled material compared to air-cooled material. Further, the phase distribution maps show that the air-cooled specimen has a significantly higher fraction of the α_2 phase compared to the slowly cooled specimen, which indicates that the former is not in thermodynamic equilibrium. The distribution of the misorientation angle between the α_2 phase in the air cooled specimen clearly exhibits peaks at around 35°, 63°, 75° and 90° (Fig. 4c), while no preferential misorientations were found for the furnace-cooled specimen (Fig. 4f). From this it can be concluded that nucleation of the α phase took place at borides in the furnace-cooled material. This explains why no misorientations according to the Burgers relationship were found and also why there was significant microstructural refinement in the furnace cooled (B-containing) alloy.
Although EBSD measurements can provide information about texture, the statistics of such measurements are relatively limited for this surface-based method. Thus to examine whether material grain refined via the heterogeneous nucleation of α phase at borides is indeed nearly free of texture within a large volume, HEXRD experiments were performed in transmission. The

investigations were carried out on sliced specimens of Ti-44.5Al-(5-7)Nb-(0.5-1)Mo-0.1B that had been used for the microstructure and EBSD analyses. In these experiments x-rays were transmitted through specimen volumes of about 1 x 1 x 3 mm^3 and the diffraction rings were recorded using a two-dimensional detector. The material volume and thus the number of grains are significantly larger than that investigated in the EBSD measurements. Fig. 5 shows the results. The recorded Debye-Scherrer diffraction rings were unrolled to lines and powder diffractograms were calculated by azimuthally integrating the patterns over an angle of 90°. The diffractograms obtained confirmed the phase constitution described above for the different heat-treated conditions, except that a few very weak reflections of the γ and β phases were detected in the oil-quenched specimens that had been heat treated in the single α-phase field. In particular, no additional phases such as borides or ω phase were evidenced in the diffractograms. Since borides were easy to find in the SEM investigations, it seems that their volume fraction was too low to be detected in the HEXRD experiments. At the position of the {100}-reflection of the ordered β phase only very weak intensity was detected, and thus it remains open whether the β phase is ordered with a B2 structure or disordered with an A2 structure.

For the as-cast specimen relatively uniform Debye-Scherrer diffraction rings for the γ, α_2 and β phases were detected (Fig. 5a). This indicates that the material has a small grain size and a weak texture. Interestingly, as marked by a circle, α_2 grains with the basal plane nearly parallel to a (110) plane of the β phase were detected, i.e. they have a Burgers orientation relationship with the remaining β phase. For the specimen heat-treated in the single α phase field, no continuous diffraction rings were observed. Rather only a very limited number of individual α_2 phase reflection spots were recorded (Fig. 5b). It therefore can be concluded that this material consists of very coarse α_2 grains. Also the material heat-treated in the α phase field, oil quenched and subsequently annealed at 1450 °C followed by air-cooling exhibited only a few reflections (Fig. 5c). These reflections however can be attributed to all three phases. For this specimen it was again observed that grains of the α_2 and β phases had a Burgers orientation relationship. In contrast, if the material was furnace cooled after annealing at 1450 °C, uniform diffraction rings from all three phases were detected (Fig. 5d). This clearly indicates that the microstructure of the material was refined within the examined macroscopic specimen volume as a result of the slow cooling rate and that the α phase formed with an almost random texture. These results confirm a grain refinement mechanism in which heterogeneous nucleation of α at borides is responsible for the grain refinement as discussed earlier for the EBSD investigations.

The results obtained by both EBSD and HEXRD have shown that microstructural refinement in furnace cooled specimens is related to the β/α transformation combined with the presence of borides and results in an apparently nearly random distribution of orientations of the α phase. However, the question arises as to why heterogeneous nucleation at borides does not generate a microstructure with a preferred orientation distribution of the α phase. According to current phase diagram information [23], β is clearly the primary solidifying phase for alloys with B contents of 0.1 at.%, with borides precipitating from the β phase. Recent work by Gosslar et al. [24] using the plane-to-plane matching model has shown that for TiAl alloys that contain 2 at. % B, the barrier for heterogeneous nucleation of the β phase on different borides is low if certain crystallographic planes of the β phase attach to certain crystallographic planes of the respective boride. Thus, it could be speculated that the reverse situation also applies and that a small nucleation barrier exists for borides precipitating from β if the same plane-to-plane matching is obeyed. Although the orientation of Borides that precipitate from the β phase might not only be determined by crystallographic matching but also by other factors as for example the nature and density of bonds across a certain interface and the strain field around the precipitate [25, 26], it appears plausible that an orientation relationship between the β and the relevant boride phase occurs as it is the case for almost all precipitation reactions. Furthermore, the work of Gosslar et al. [24] also indicated a low barrier for heterogeneous nucleation of α phase at the boride phases TiB_2 with the C32 structure and TiB with the B27 structure, combined with the associated preference for certain crystallographic matching planes in the α and boride phase. This means that if the α phase is nucleated at borides during the β/α transformation, then a crystallographic orientation relationship between the parent β phase, the boride phase and the α phase should exist. Because β dendrites grow preferentially with a <100> orientation parallel to the heat flow during solidification [6, 27], preferred orientations of the α phase and thus, of the α_2 and γ lamellae should result. This was neither observed in the present study nor by Hecht et al. [5] who argued that the α phase is nucleated at borides that formed in the prior interdendritic regions of the melt and thus do not exhibit any preferred orientation. This however does not explain why nucleation of α phase at borides that are inside prior dendrites does not occur or does not generate preferred orientations. In the following section information about the types of borides present in the alloys investigated and an explanation why preferred orientations do not occur for heterogeneous α nucleation at borides in primary β dendrite cores is presented.

In order to identify the crystal structure of the borides present in the as-cast condition, EBSD investigations were conducted on a specimen of the Ti-44.5Al-(5-7)Nb-(0.5-1)Mo-0.1B alloy (Fig. 6). Crystallographic data according to the publication of De Graef et al. [28] is given (Table 1) for the four boride phases that have up to now been found in TiAl alloys [29]. The investigations comprised long straight boride ribbons as well as borides with "blocky" morphology. The borides with a curved ribbon morphology that were observed in interdendritic regions were not examined. It was found that EBSD analysis could not distinguish between the TiB_2 phase with the hexagonal C32 structure and the hexagonal α_2 phase, thus its existence remains open. However, as shown in Fig. 6 monoborides of the B27 and B_f structures were identified, exhibiting either a long straight appearance or a blocky form. It was not investigated if different morphologies of Borides existed or whether they arose from the same long straight boride shape intersecting the specimen surface at different orientations. Similarly, Hill et al. [21] identified the occurrence of the TiB phase with B27 structure in B-containing Ti alloys based on Ti-6Al-4V and Hu et al. [30] in the Ti aluminide alloy Ti-44Al-8Nb-0.1B. In both studies the orientation relationship {011}β || (001)B27 and <111>β || [010]B27 was determined between the β and the adjacent TiB phase. Interestingly, Hill et al. [21] found that refined equiaxed grains of the α phase were observed after slow cooling from the β phase field, while on faster cooling the β phase adopted a Widmannstätten lath-like microstructure. Assuming that monoborides with the B27 structure were precipitated from the β phase, this would result in 12 possible orientations of TiB in one β grain according to the above orientation relationship. If during the β/α transformation the α phase is heterogeneously nucleated at the boride particles, then a certain number of α phase orientations might occur with respect to the TiB phase. Hill et al. [21] as well as Hu et al. [30, 31] observed the orientation relationship (0001)α || (001)B27 and <11-20>α || [010]B27, which would result in the Burgers orientation between the β and the α phases. However, the orientation relationships [0-111]α || [-104]B27 and [2-1-10]α || [010]B27 [32] as well as (1-101)α || (001)B27, (11-20)α || (010)B27 and (1-10-2)α || (100)B27 [33] have also been found in a boron containing Ti alloy. Thus, a large number of α phase orientations might be generated if the α phase is nucleated at a TiB (B27) particle precipitated from the β phase. The number of possible α phase orientations could even be further increased by the presence of borides with different crystal structure within the alloy, as e.g. the TiB phase with B_f structure that has been identified in the alloy. This can explain why heterogeneous nucleation of the α phase at borides also inside prior β dendrites generates a nearly random distribution of orientations.

It is indeed somewhat surprising that microstructural refinement is obtained for slow rather than for fast cooling. In a formal manner this means that the TTT curve of the β/α transformation is shifted to higher temperatures and longer times as a result of heterogeneous nucleation of the α phase at borides. It seems evident that heterogeneous nucleation at inoculants would raise the start temperature of the transformation. However, the reason why the formation of Widmannstätten α-laths proceeds faster than the precipitation of equiaxed α grains during the β/α transformation remains to be explained. In general, the growth of Widmannstätten lath structures follows the kinetics of discontinuous precipitation reactions, while equiaxed precipitates grow according to the time law of spherical precipitates. Both precipitation reactions can be controlled by the kinetics of diffusional transport or by the interface mobility. At the present stage the various factors involved in the kinetics of the two reaction types are not known and thus, nothing can be concluded with respect to the velocity of the competing transformations. An analysis of the growth kinetics requires further experimental work, which could performed either in-situ at the transformation temperature, e.g by employing dilatometry or HEXRD, or could involve metallography of specimens rapidly quenched from different intermediate states of a heat treatment cycle.

Finally, it is worth noting that the as-solidified microstructure of the B-containing alloys is finer than observed in the B-free alloys and does not exhibit significant preferred crystal orientations. Since the cooling rate during solidification is certainly considerably higher than on furnace cooling as becomes evident by comparing the lamellae thicknesses (cf. Fig. 4 d, e and Fig. 6), this effect cannot be understood by the influence of Borides on the β/α transformation. Rather, this observation indicates that B additions also affect the solidification microstructure before the β/α transformation begins. Hu et al. [31] performed directional solidification experiments followed by rapid quenching. In this way the microstructure and texture directly after solidification could be made visible. In the experiments solidification occurred at a cooling rate of 100 K/min prior to quenching, i.e. the cooling rate was roughly the same as applied during furnace cooling in the present work. Hu et al. [31] observed that the addition of 1 at.% B to the alloy Ti-45Al-2Nb-2Mn significantly reduced the size of β dendrites compared to the B-free counterpart. This result was explained by the pronounced partitioning of B to the melt during solidification which induces strong constitutional undercooling in the segregation zone and an increased number of nucleation events as first suggested by Cheng [17]. After solidification a relatively fine and weakly textured β-grain structure was formed. Thus, the subsequent β/α transformation will likewise generate a fine microstructure without significant preferred orientations, irrespective of the mode of the

transformation. If the microstructure of such a material is coarsened by a heat treatment, subsequent microstructural refinement through the β/α transformation in a further heat treatment would require however relatively slow cooling as shown above. In a further study Hu et al. [30] investigated the microstructure formation of the alloy Ti-44Al-8Nb-1B during directional solidification under the same experimental conditions and concluded, that grain refinement in this material occurred due to boride-assisted α phase nucleation during the β/α transformation. Since the cooling rate during solidification again was similar to that applied by furnace cooling in the present work, the conclusion agrees with our results. However, the heterogeneous nucleation at borides in the β/α transformation does not exclude that prior to this transformation a fine and texture-free β-grain structure was present. Here it is worth mentioning that heterogeneous nucleation of the α phase at borides and a resulting grain refinement were observed for fast cooling rates in a B containing Ti alloy based on Ti-6Al-4V [34]. However, in this case the β/α transformation occurred directly after solidification without heat treatment. After heat treatments grain refinement in this material was only found after slow cooling [21] as already noted above. This indicates in agreement with the present work that the grain refinement mechanism operating during solidification and subsequent cooling differs from that active during cooling after heat treatments in the β phase field.

4 Conclusions

It has been shown that for β-solidifying γ-titanium aluminide alloys with low B additions significant microstructural refinement can be obtained by a heat treatment in the β single-phase region followed by slow cooling. This effect is not related to the solidification of the primary β phase and has been clearly attributed to the presence of borides in the alloys. Borides act as inoculants for the α phase and favour the precipitation of equiaxed α grains from the β phase on account of the formation of Widmannstätten α-laths. The microstructural refinement effect generates an almost random orientation distribution of the α phase and thus of the γ lamellae that subsequently precipitate from the α phase. This has been attributed to the nucleation of α phase at borides formed within interdendritic regions of the melt or to the large number of possible α phase orientations available when nucleation takes place at borides that precipitated at higher temperatures from the β phase. While it is evident from the investigation that heterogeneous nucleation of α phase at borides is promoted by slower cooling rates and suppressed by high cooling rates, the reasons for this are not yet understood.

Acknowledgments

The authors thank U. Lorenz and S. Eggert (HZG, Geesthacht) for continuous experimental advice and support, and F. Appel, H. Gabrisch (HZG, Geesthacht), U. Hecht (ACCESS, Aachen), D. Gosslar (TU Hamburg-Harburg), S. Gebhard, D. Roth-Fagaraseanu, and S. Kötzsch (Rolls-Royce Deutschland Ltd, Dahlewitz) for stimulating discussions. Financial support by Rolls-Royce Deutschland Ltd and the Ministry for Economy of the Federal State Brandenburg within the Joint Project "PräziTal" and by the German Research Foundation (DFG) within the priority programme SPP 1296 (project PY 69/2-2) is gratefully acknowledged.

References

[1] Kim Y-W, Dimiduk DM. In: Nathal MV, Darolia R, Liu CT, Martin PL, Miracle DB, Wagner R, Yamaguchi M, editors. Structural Intermetallics 1997. Warrendale (PA): TMS, 1997, pp. 531-543.
[2] Appel F, Wagner R. Mater. Sci. Eng. R 1998; R22: 187-268.
[3] Wu X. Intermetallics 2006; 14: 1114-1122.
[4] Loretto MH, Wu Z, Chu MQ, Hu D. In: Palm M, Bewlay BP, Kumar KS, Yoshimi K, editors. Intermetallic-Based Alloys for Structural and Functional Applications, Mater. Res. Soc. Symp. Proc, Vol. 1295. Warrendale (PA): MRS, 2011, pp. 85-94.
[5] Hecht U, Witusiewicz V, Drevermann A, Zollinger J. Intermetallics 2008; 16: 969-978.
[6] Naka S, Thomas M, Sanchez C, Khan T. In: Nathal MV, Darolia R, Liu CT, Martin PL, Miracle DB, Wagner R, Yamaguchi M, editors. Structural Intermetallics 1997. Warrendale (PA): TMS, 1997, pp. 313-322.
[7] Johnson DR, Inui H, Yamaguchi M. Intermetallics 1998; 6: 647-652.
[8] Küstner V, Oehring M, Chatterjee A, Clemens H, Appel F. In: Herlach D, editor. Solidification and Crystallization. Weinheim: WILEY-VCH, 2004, pp. 250-257.
[9] Imayev RM, Imayev VM, Oehring M, Appel F. Intermetallics 2007; 15: 451-460.
[10] Cheng TT, Loretto MH. Acta Mater. 1998; 46: 4801-4819.
[11] Takeyama M, Ohmura Y, Kikuchi M, Matsuo T. Intermetallics 1998; 6: 643-646.
[12] Zhang Z, Leonard KJ, Dimiduk DM, Vasudevan VK. In: Hemker KJ, Dimiduk DM, Clemens H, Darolia R, Inui H, Larsen JM, Sikka VK, Thomas M, Whittenberger JD, editors. Structural Intermetallics 2001. Warrendale (PA): TMS, 2001, p. 515-526.
[13] Jin Y, Wang JN, Yang J, Wang Y. Scripta Mater. 2004; 52: 113-117.

[14] Appel F, Oehring M, Paul JDH. Adv. Eng. Mater. 2006; 8: 371-376.
[15] Clemens H, Chladil HF, Wallgram W, Zickler GA, Gerling R, Liss K-D, Kremmer S, Güther V, Smarsly W. Intermetallics 2008; 16: 827-833.
[16] Larsen DE, Christodoulou L, Kampe SL, Sadler P. Mater. Sci. Eng. A 1999; A144: 45-49.
[17] Cheng TT. Intermetallics 2000; 8: 29-37.
[18] Hu D. Intermetallics 2001; 9: 1037-1043.
[19] Banerjee S, Mukhopadhyay P. Phase Transformations – Examples from Titanium and Zirconium Alloys. Pergamon Materials Series, Vol. 12, Amsterdam, The Netherlands: Elsevier, 2007.
[20] Hu D, Jiang H, Wu X. Intermetallics 2009; 17: 744-748.
[21] Hill D, Banerjee R, Huber D, Tiley J, Fraser HL. Scripta Mater. 2005; 52: 387-392.
[22] Gey N, Humbert M. Acta Mater. 2002; 50: 277-87.
[23] Witusiewicz VT, Bondar AA, Hecht U, Zollinger J, Artyukh LV, Velikanova TYa. J. Alloys Comp. 2009; 474: 86-104.
[24] Gosslar D, Hartig C, Günther R, Hecht U, Bormann R. J. Phys. Condens. Matter 2009; 21: 464111 (7pp).
[25] Zhang W-Z, Weatherly GC. Progr. Mater. Sci. 2005; 50: 181-292.
[26] Zhang M-X, Kelly PM. Progr. Mater. Sci 2009: 54: 1101_1170.
[27] Johnson DR, Chihara K, Inui H, Yamaguchi M. Acta Mater. 1998; 46: 6529-6540.
[28] De Graef M, Löfvander JPA, McCullough C, Levi CG. Acta Metall. Mater. 1992; 40: 3395-3406.
[29] Kitkamthorn U, Zhang LC, Aindow M. Intermetallics 2006; 14: 759-769.
[30] Hu D, Yang C, Huang A, Dixon M, Hecht U. Intermetallics 2012; 23: 49-56.
[31] Hu D, Yang C Huang A, Dixon M, Hecht U. Intermetallics 2012; 22: 68-76.
[32] Genç A, Banerjee R, Hill D, Fraser HL. Mater. Lett. 2006; 60: 859-863.
[33] Banerjee R, Genç A, Hill D, Collins PC, Fraser HL. Scripta Mater. 2005; 53: 1433-1437.
[34] Banerjee R, Collins PC, Genç A, Faser HL. Mater. Sci. Eng. A 2002; A358: 343-349.

Designation	Struktur-bericht	Space group	Pearson symbol	Prototype	Lattice parameters (Å)	Wyckoff positions/fractional coordinates				
TiB_2	C32	P6/mmm	hP3	AlB_2	a = 3.03	Ti	1a	0	0	0
	No. 191				c = 3.23	B	2d	0.333	0.667	0.5
TiB	B27	Pnma	oP8	FeB	a = 6.11	Ti	4c	0.127	0.25	0.123
		No. 62			b = 3.05	B	4c	0.029	0.25	0.603
					c = 4.56					
TiB	B_f	Cmcm	oC8	CrB	a = 3.23	Ti	4c	0	0.146	0.25
		No. 63			b = 8.56	B	4c	0	0.44	0.25
					c = 3.05					
Ti_3B_4	$D7_b$	Immm	oI14	Ta_3B_4	a = 3.26	Ti	2c	0.5	0.5	0
		No. 71			b = 13.73	Ti	4g	0	0.18	0
					c = 3.04	B	4g	0	0.375	0
						B	4h	0	0.444	0.5

Table 1. Crystallographic data for various borides that occur in TiAl alloys, De Graef et al. [28].

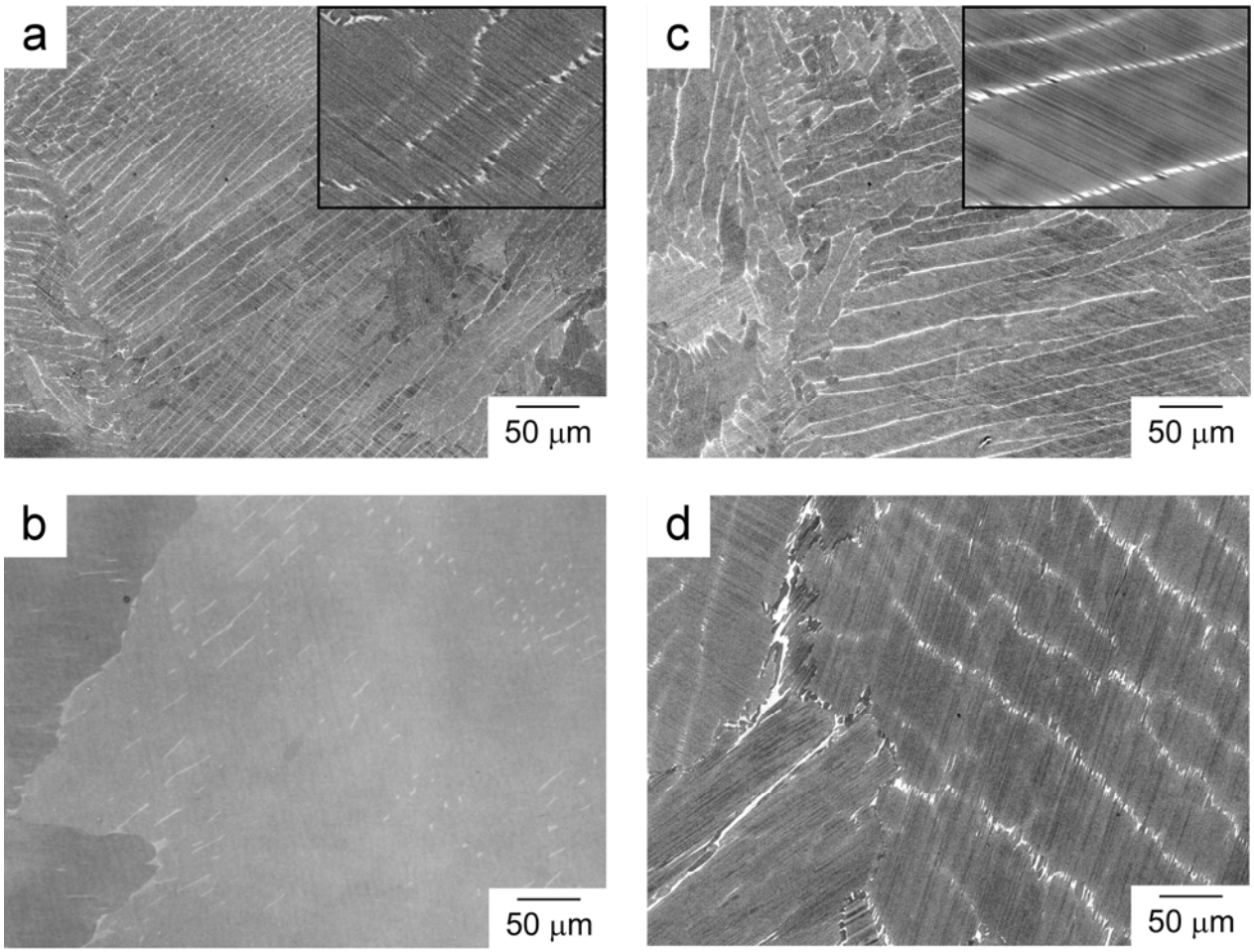

Fig. 1. Scanning electron micrographs, taken in the back-scattering electron mode, of the alloy Ti-45Al-7Nb-1Mo. (a) As-cast condition, (b) heat-treated 2 h at 1310 °C/oil quenched, (c), (d) heat-treated 2 h at 1310 °C/oil quenched and subsequently heat-treated 1h at 1450 °C and (c) air cooled or (d) furnace cooled. The insert in (c) shows a section of the image area in higher magnification.

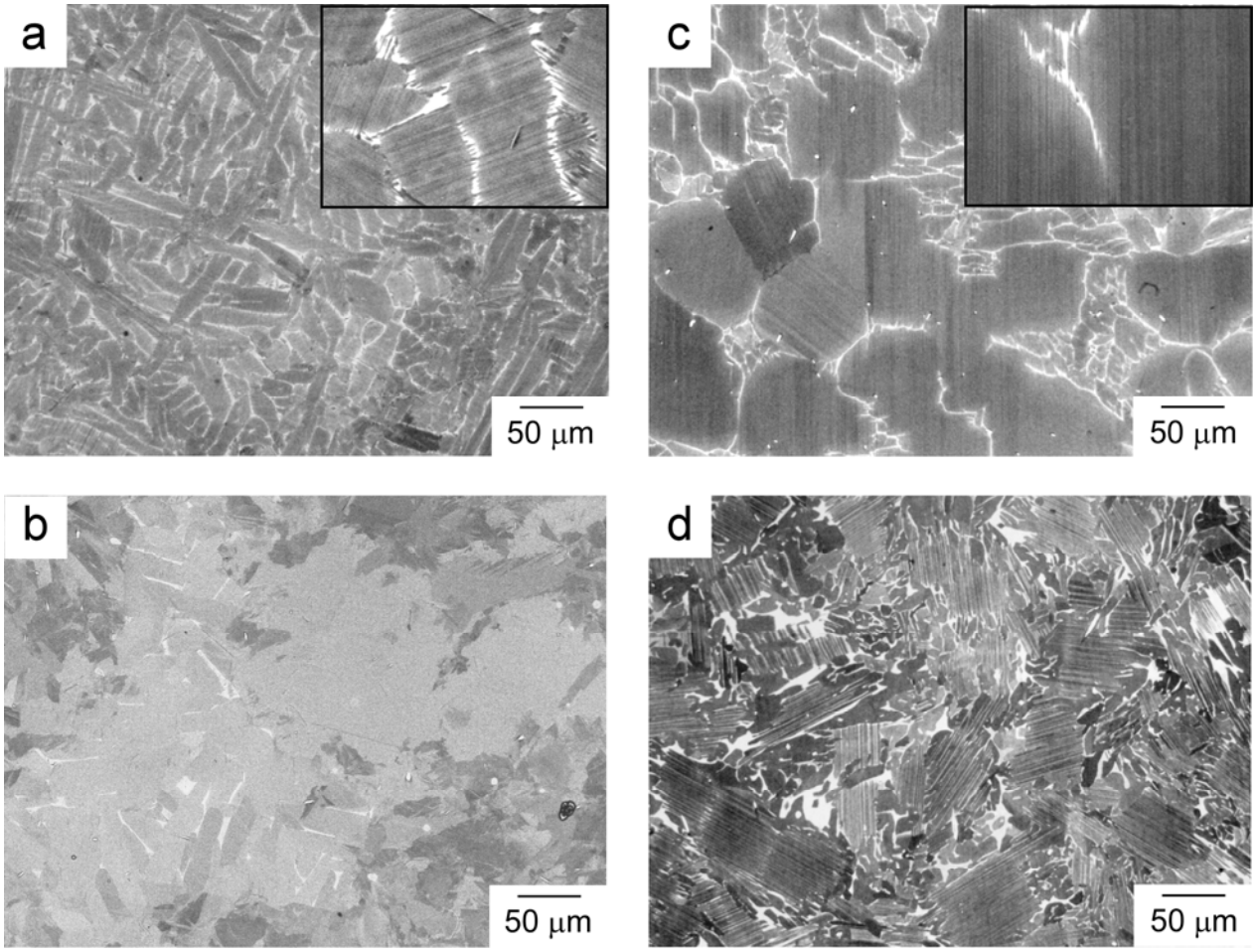

Fig. 2. Scanning electron micrographs, taken in the back-scattering electron mode, of the alloy Ti-45Al-7Nb-1Mo-0.1B. (a) As-cast condition, (b) heat-treated 2 h at 1310 °C/oil quenched, (c), (d) heat-treated 2 h at 1310 °C/oil quenched and subsequently heat-treated 1h at 1450 °C and (c) air cooled or (d) furnace cooled.

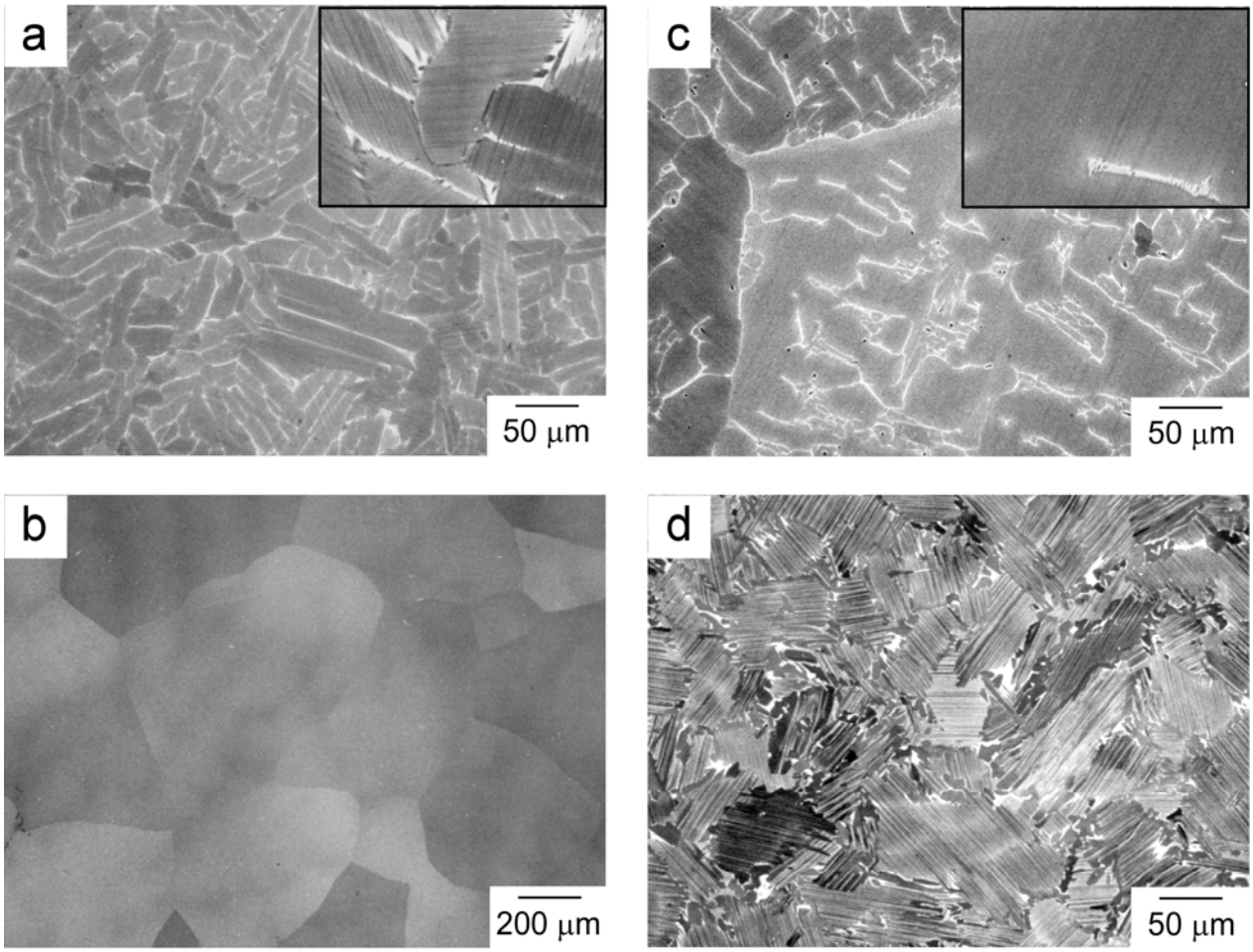

Fig. 3. Scanning electron micrographs, taken in the back-scattering electron mode, of the alloy Ti-44.5Al-(5-7)Nb-(0.5-1)Mo-0.1B. (a) As-cast condition, (b) heat-treated 2 h at 1310 °C/oil quenched, (c), (d) heat-treated 2 h at 1310 °C/oil quenched and subsequently heat-treated 1h at 1450 °C and (c) air cooled or (d) furnace cooled.

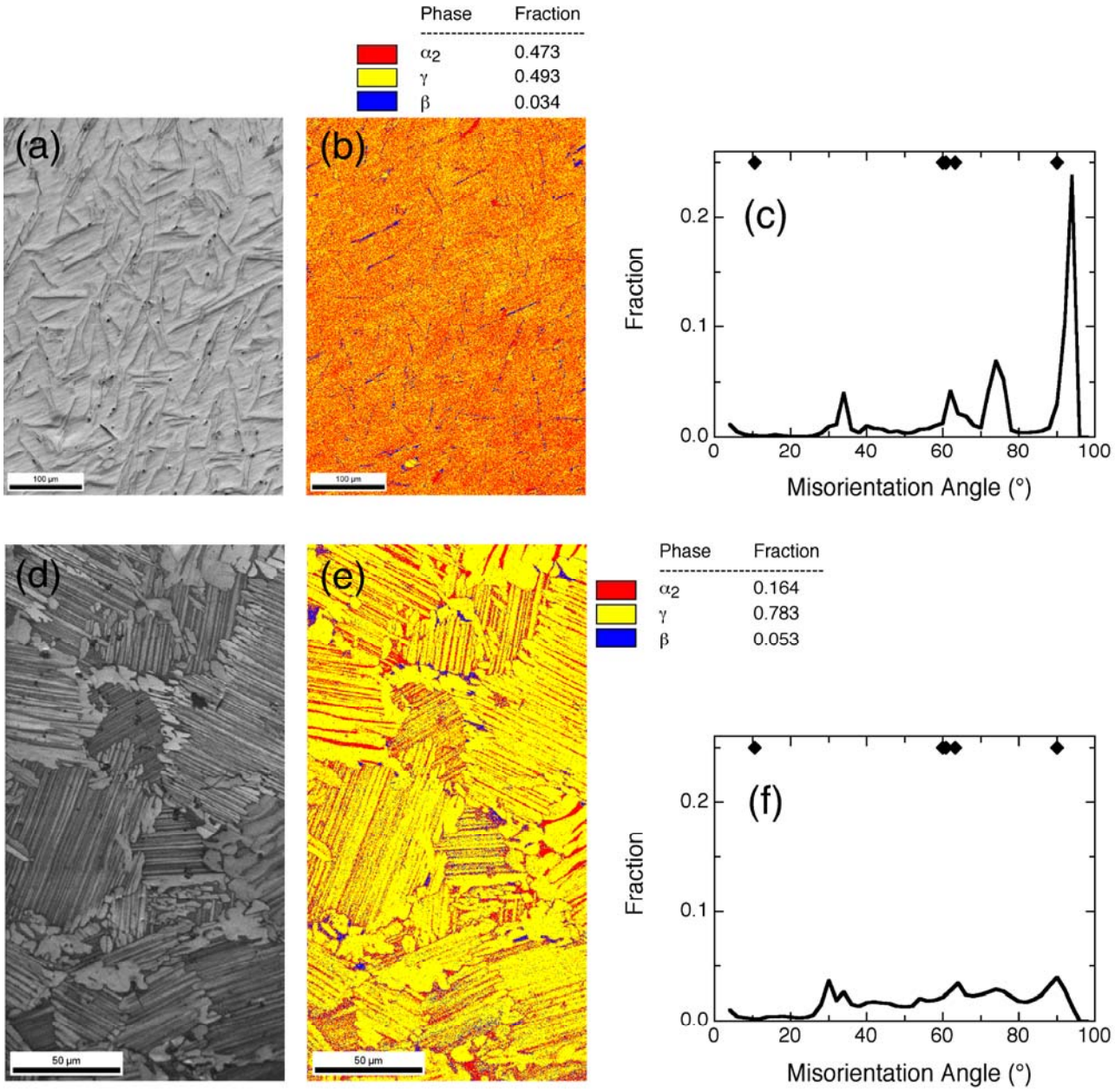

Fig. 4. Results of EBSD investigations on the alloy Ti-44.5Al-(5-7)Nb-(0.5-1)Mo-0.1B. (a), (b), (c): material heat-treated 2 h at 1310 °C/oil quenched and subsequently heat-treated 1h at 1450 °C/air cooled, (d), (e) and (f): material heat-treated 2 h at 1310 °C/oil quenched and subsequently heat-treated 1h at 1450 °C/furnace cooled. (a), (d): Image quality maps, (b) and (e): phase maps, (c), (f) misorientation angle distribution for the α_2 phase. The diamond symbols indicate the misorientations that occur between orientation variants originating from one parent β grain according to the Burgers orientation relationship.

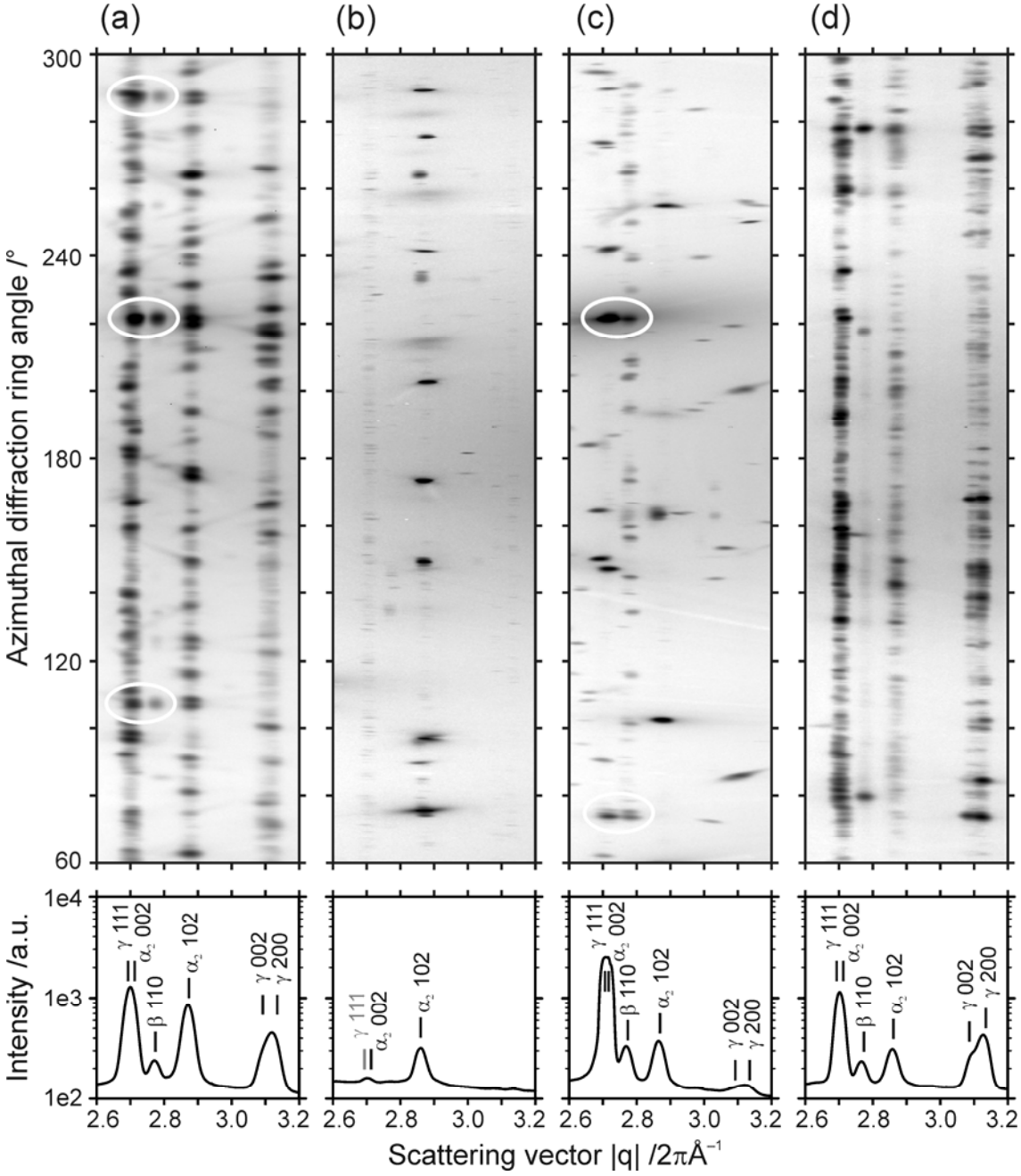

Fig. 5. X-ray diffraction patterns of Ti-44.5Al-(5-7)Nb-(0.5-1)Mo-0.1B in (a) as-cast condition, (b) heat-treated 2 h at 1310 °C/oil quenched, (c), (d) heat-treated 2 h at 1310 °C/oil quenched and subsequently heat-treated 1h at 1450 °C and (c) air cooled or (d) furnace cooled. The Debye-Scherrer diffraction rings have been unrolled to lines as well as azimuthally integrated, thus resulting in a typical powder diffraction pattern. The white circles in the diffraction patterns indicate reflection pairs that correspond to the Burgers orientation relationship.

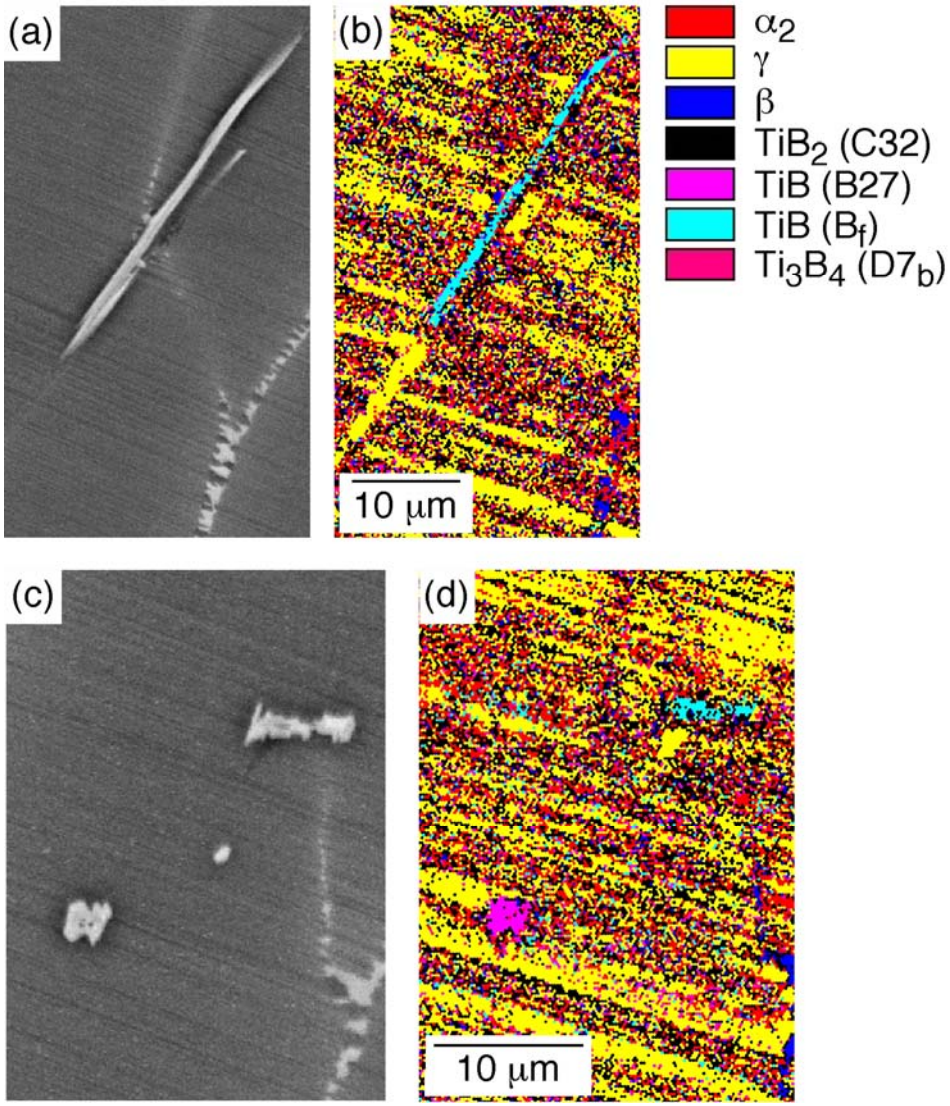

Fig. 6. Results of EBSD investigations on the alloy Ti-44.5Al-(5-7)Nb-(0.5-1)Mo-0.1B in the as-cast condition. (a), (c): SEM micrographs (BSE mode) and (b), (d): corresponding EBSD phase map.